

# COMPLETENESS OF MEASUREMENTS OF THE ORBITAL DEBRIS ENVIRONMENT

Gene Stansbery<sup>(1)</sup>, J. L. Foster, Jr.<sup>(2)</sup>

<sup>(1)</sup>NASA Johnson Space Center, 2101 NASA Parkway, Mail Code KX, Houston, TX, 77058, USA,  
Email: eugene.g.stansbery@nasa.gov

<sup>(2)</sup>ESC Group, PO Box 58447, Mail Code JE104, Houston, TX, 77258, USA,  
Email: james.l.foster1@jsc.nasa.gov

## ABSTRACT

A great amount of effort has gone into making measurements of the orbital debris environment using a variety of methods and instruments. The aggregate of measurements provides a good overall characterization of the environment. However, each instrument or technique has inherent limitations. *In situ* measurements using returned surfaces, such as LDEF, are limited by finite surface area and discrete altitudes and time on orbit. Statistical measurements using radars and telescopes are limited by sensitivity and geographical location. The U.S. Space Surveillance Network catalog is incomplete since it also relies on radar and optical measurements as well. Understanding the limitations with each technique can provide insight into the limitations in the broad characterization of the debris environment. This paper will explore the major limitations of individual measurement techniques and their implications for understanding the overall orbital debris environment.

## 1. INTRODUCTION

Measurements are the cornerstone of space debris modeling, mitigation and risk assessment. Many techniques are used to measure the environment including remote sensing with optical and radar instruments and impact detectors or returned surfaces. No single measurement technique gives a complete picture of the environment. Each has its own strengths and weaknesses. Even taken collectively, measurements do not provide total knowledge of environment. Gaps in altitude coverage, sensitivity, and incomplete orbital elements will continue for the foreseeable future.

## 2. STARING RADARS

Research radars operated in a staring mode, where the antenna is pointed at a fixed azimuth and elevation while debris objects pass through the field-of-view, have proven to be very useful for statistical measurements of the space debris environment. The Haystack, Haystack Auxiliary, Goldstone, and FGAN/TIRA radars all operate in this mode for debris measurements. The Haystack radar has

accumulated the most debris collection time in this mode.

Haystack is a high power, X-band (3-cm wavelength), monopulse tracking radar with very high sensitivity. To detect debris, a pulsed, single frequency waveform is used. The single pulse signal-to-noise ratio on a 1-m<sup>2</sup> target at 1000 km range is 56.8 dB using a 1.023 msec pulse. When Haystack is operated in a staring mode, a very simple detection algorithm is used. During operation, a real-time processing and control system (PACS) arranges the received data into overlapping range gates. It then transforms each range gate into frequency space and keeps a running 12-pulse non-coherent integration of each range-Doppler cell. If any cell exceeds a preset threshold, detection has occurred and all data associated with the detection is saved. At this point, saved detections include side-lobe detections, noise detections, and of course, main-lobe detections of resident space objects (RSOs).

Post-processing is performed which is intended to eliminate all side-lobe detections and to reduce the number of noise detections to a small fraction (typically 1-2 %) of the number of real detections of RSOs. During post processing, the radar cross section (RCS) is determined by the signal strength and the range to the object with corrections based on the estimated path through the radar beam. The RCS is related to size from NASA's Size Estimation Model (SEM).

Fig. 1 shows debris data collected from October 2001 – September 2002 from Haystack at a staring angle of 75° elevation, and 90° azimuth. In order to cover the altitude range of interest, the data in this figure was collected in two separate range windows. 171 hours were collected using a range window of 312-1297 km and 175 hrs were collected with a range window of 1030-2015 km. At the lowest altitudes (300-500 km), debris as small as 2-3 mm diameter are detected while at the highest altitudes (1700-1900 km), the smallest detection is in the 6-7 mm range. This lower detection limit as a function of altitude is consistent with the 1/range<sup>4</sup> power law inherent in the radar range equation. It indicates that range is the dominant factor in probability-of-detection calculations for this detection algorithm, although it is not the only factor.

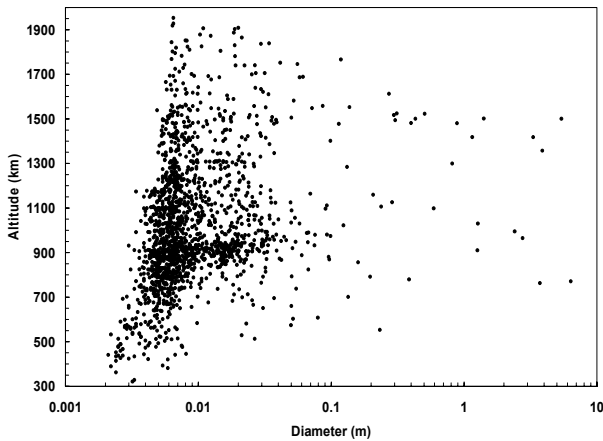


Figure 1. Debris data collected from October 2001 – September 2002 from Haystack at a staring angle of  $75^\circ$  elevation, and  $90^\circ$  azimuth. In order to cover the altitude range of interest, the data in this figure was collected in two separate range windows. 171 hours were collected using a range window of 312–1297 km and 175 hrs were collected with a range window of 1030–2015 km.

At low altitudes, debris passes through the radar beam in only 3 or 4 pulses while the return signal from 12 pulses is used for non-coherent integration. This means that 8 or 9 noise or sidelobe returns are also integrated thus lowering the signal-to-noise ratio (SNR) upon which detection is determined. A more sophisticated detection algorithm would choose the number of pulses to integrate based on altitude, but it is expected that the gain in sensitivity would be minimal and it has not yet been implemented.

For a given altitude in Fig. 1, the probability-of-detection (Pd) decreases from near 100% to near 0% as smaller sizes are examined. A computer model was generated to predict this decrease in Pd. The model calculates the average probability-of-detection for a given debris size and slant range. The RCS of an object of given size is estimated using the NASA Size Estimation Model. The program initially calculates the trajectory of an object through the center of the radar beam. The model considers 12 points along the trajectory spaced appropriately to emulate the individual radar return pulses given the pulse repetition frequency (PRF) of the radar and altitude of the object (assuming a circular orbit). The model calculates the SNR of each of the points corrected for the antenna gain at each point's location. It then integrates the SNR from the 12 points and calculates the probability-of-detection (Pd) for the trajectory for different scintillation models. The model repeats the Pd calculations for as many as 100 parallel trajectories, uniformly sampling the detection area from beam center to the edge of the main beam.

Fig. 2 shows example results of Pd as a function of size for non-fluctuating targets for Haystack data using the 1.023 millisecond waveform (Foster, 2005).

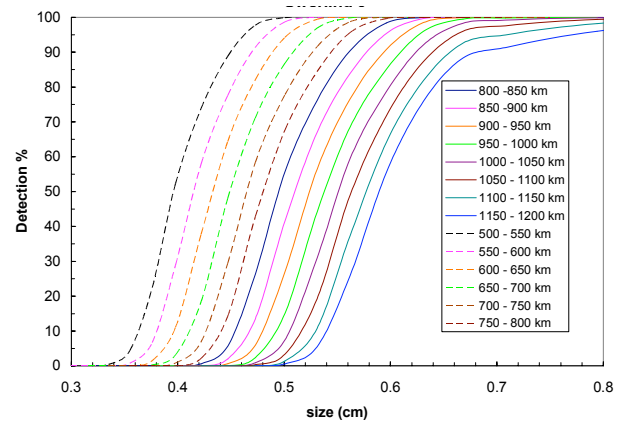


Figure 2. Probability-of-detection as a function of size for non-fluctuating targets for Haystack data using the 1.023 millisecond waveform.

### 3. STARING OPTICAL TELESCOPES

Optical instruments operating in staring mode, such as NASA's Liquid Mirror Telescope (LMT) will produce similar probability-of-detection issues as radars. Rather than a  $1/\text{range}^4$  detection limitation optical detection should follow a  $1/\text{range}^2$  pattern. The LMT used a 3-m diameter main mirror created by spinning liquid mercury in a parabolic dish. The sensor was a commercial digital video camcorder image of a Gen II microchannel plate. This produced a compressed 720x640 pixel video at 29.97 frames per second, video rate (Africano, 1999). An elaborate automated streak detection algorithm was developed. The algorithm created a library of matched filters for comparison with each image after subtraction of the star and average noise background. The algorithm then found the maximum matched filter output for each of seven altitude bins. The rate that an image crossed the field-of-view was related to the object's altitude assuming circular orbits. In practice, the crossing rate for low altitude debris (<600 km) was indistinguishable from the horizontal rate of many meteor streaks. NASA's experience was that below 600 km, the flux of meteor trails was higher than the flux of orbital debris negating the extraction of useful debris information.

At near geosynchronous altitudes, CCD detectors are normally used. In this case, SNR depends on the sensitivity of the detector, the length of the exposure, the number of pixels the satellite signal is spread over, and how much background light or noise is contained in each pixel. In addition, there is also the issue of clutter from background stars. To maximize the SNR, the size of the image should exactly match the pixel size. In this

way, the signal is maximized for the background noise. In practice, the signal is typically spread over several pixels. For instance, objects with different orbital inclinations will have different north-south velocity components. The telescope, or the image on the CCD, can be slewed at a selected orbital rate to match the motion of the satellite in order to concentrate all of the light onto a single pixel. However, the search strategy can only be optimized for one inclination at a time. All other inclinations have a lower SNR and hence probability-of-detection.

#### 4. PHASED ARRAY RADAR

Phased array radars operate differently from Haystack in that they are electronically steered without physically moving the radar antenna. This means that the antenna beam can be instantaneously moved within some angular limits. What is typically done with phased array radars is to rapidly move the beam in a long, narrow pattern to create a virtual fan beam, or fence. While maintaining the fence, some radar time and transmit power is typically allocated for tracking of objects detected by the fence.

Cobra Dane is a phased array radar used by the U.S. for debris measurements. It is located on Shemya Island, Alaska at 52.7° N latitude and 174.1° E longitude. Cobra Dane is an L-band (23-cm wavelength) radar which first became operational in 1977. The radar generates approximately 15.4 MW of peak RF power (0.92 MW average) from 96 Traveling Wave Tube (TWT) amplifiers arranged in 12 groups of 8. This power is radiated through 15,360 active array elements. The face of the radar is aligned at an azimuth of 319°.

Phased array radars such as Cobra Dane typically have a more complicated detection scheme than that is used at Haystack. Rather than integrating a number of pulses, initial detection is based on the return signal exceeding a preset threshold on a single pulse. This results in a large number of false alarms. When an initial detection is sensed, a second, confirming transmit pulse is sent at the same location in the fence. If the threshold is exceeded on the second pulse, then the radar attempts to track the object. If the object is scintillating, the threshold might not be crossed on every pulse. An object will remain in track only if a sufficient fraction of the pulses exceed the threshold. This is sometimes called an “ $n$  out of  $m$ ” detection algorithm.

Fig. 3 shows the results from Cobra Dane collected during the IADC 24-hour campaign conducted in September 2004. During the campaign, a 40° wide fence was erected at an elevation of 50.3° and centered in azimuth at the boresight. During the campaign, 3400 objects were detected crossing the fence. Of these detections, ~300 objects were seen more than once,

leaving 3100 unique objects. Unlike the corresponding Haystack plot, no  $1/\text{range}^4$  detection limit is apparent in Fig. 3. Instead, at least below 1300 km, the lower limit of detections is about 4 cm diameter. This is an operational choice included in the software that controls the radar and is not a function of the detection capability of the radar.

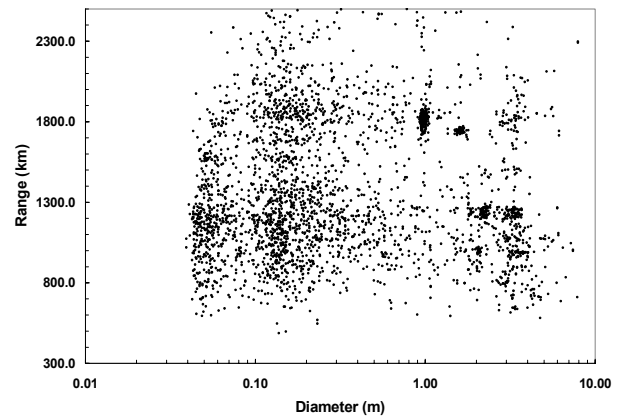


Figure 3. Results from Cobra Dane collected during the IADC 24-hour campaign conducted in September 2004. During the campaign, a 40° wide fence was erected at an elevation of 50.3° and azimuth of 299°–339°.

Another complication inherent in phased array radars is the availability of radar resources. This is basically a time and power management issue. In order to create the detection fence, the radar is pointed in 100 different locations. At each location a 1500  $\mu\text{sec}$  pulse is transmitted. Then the beam remains pointed in that location for the time it takes the radar pulse to make the round trip to the top of the receive window, ~17 msec for the maximum slant range of 2500 km. Each location in the fence is nominally revisited every four seconds. However, if any objects are being tracked, then additional time and transmit power are needed to maintain the tracking of the object. If several objects are being tracked simultaneously, there may not be time or transmit power available to maintain every location on the fence. Apparently this situation occurred during the 24-hour campaign. During the 2004 24-hour campaign, only about 90% of the cataloged objects predicted to pass through the Cobra Dane fence (using orbit propagation software and current element sets) were actually detected and reported.

#### 5. RETURNED SURFACES

Information on very small debris often comes from examination of returned surfaces such as the Long Duration Exposure Facility (LDEF) or the Hubble Space Telescope solar panels. Returned spacecraft surfaces are examined for craters or holes caused by hypervelocity impacts. Debris (both man-made and natural) size is estimated from the hole or crater size.

For returned surfaces, there are practical limitations on both ends of the size spectrum. Typically, when spacecraft material is returned, an optical microscope is used to scan the entire exposed surface for visible holes or craters. Selected areas are often scanned using higher magnification such as scanning electron microscopes. Ultimately at the smallest sizes, the inherent limitation is that impact features will be indistinguishable from surface irregularities.

At the other end of the size spectrum, returned surfaces are limited by their size and the duration of their exposure to the debris environment. The expected number of impacts on a space-exposed surface is proportional to the area of the surface, the time it was exposed, and the debris flux. Assuming Poisson statistics, the probability,  $P(N,X)$ , of observing exactly  $N$  events, where  $X$  is the expected event rate, is given by:

$$P(N,X) = e^{-X}(X^N/N!) \quad (1)$$

The uncertainty for the few largest detections is quiet large. For example, the largest impact feature on LDEF was an approximately 5 mm diameter crater that impacted one of the aluminum trusses which made the frame for the experiment trays. This was estimated to have been caused by a man-made debris object about 1 mm diameter. (LDEF spent 5.7 years in orbit from April 1984 to January 1990 at altitudes from ~500 km at deployment to ~375 km at retrieval.) At the 95% confidence level, the flux derived from that 1 impact could have been 0.0253 times the flux up to 7.22 times the flux. Table 1 gives the 90%, 95%, and 99% confidence limits on  $X$  for a given  $N$  for up to 10 detections (Ricker, 1937). For debris larger than the largest size detected, the fact that no impacts were found sets an upper limit to the measured (or in this case unmeasured) flux.

Table 1. Confidence limits on detection rate  $X$  for a given number of detections  $N$ .

N	Confidence Limits					
	99%		95%		90%	
1	0.00501	7.43	0.0253	5.57	0.0513	4.74
2	0.1035	9.27	0.242	7.22	0.355	6.3
3	0.338	10.98	0.619	8.77	0.818	7.75
4	0.672	12.59	1.09	10.24	1.37	9.15
5	1.08	14.15	1.62	11.67	1.97	10.51
6	1.54	15.66	2.2	13.06	2.61	11.84
7	2.04	17.13	2.81	14.42	3.29	13.15
8	2.57	18.58	3.45	15.76	3.98	14.43
9	3.13	20	4.12	17.08	4.7	15.7
10	3.72	21.4	4.8	18.39	5.43	16.96

## 6. SPACE SURVEILLANCE NETWORK CATALOG

Both the U.S. and Russia operate space surveillance networks and maintain catalogs of RSOs and their

orbital elements. For the U.S., tracked objects are maintained in two lists. Each list has its own completeness issues. Objects in the official catalog are given, along with their international designator, a sequential number starting with satellite number 1, the Sputnik 1 rocket body. Currently there are over 28,000 objects in the regular catalog including close to 19,000 objects which have reentered the Earth's atmosphere or have left Earth orbit. The criteria for inclusion in the official catalog are that the object be reliably tracked and that the object is associated with a launch. COSPAR convention does provide for assignment of an international designator without identification of associated launch. However, there is only one debris object in the U.S. catalog, 1977-000E, which does not have an associated launch. This is a piece of debris that is in an orbit that only the U.S. has launched satellites into. Therefore its country of origin can be reliably identified, if the specific launch cannot.

Objects which are routinely tracked by the U.S. SSN but which have not yet been identified by mission are maintained in an "Analyst" list using numbers from 80,000 to 89,999. Objects in the analyst catalog are often transient in that they are discovered, tracked, identified, and then transferred to the regular catalog. The number in the analyst catalog is then reused. Many objects in the analyst list reenter or are administratively removed prior to them entering the regular catalog. Since objects in the analyst list do not have to have an associated launch, the completeness of this list is primarily driven by the probability-of-detection issues at individual optical and radar sensors that make up the SSN.

However, operational procedures still have an impact. For example, the Air Force conducted a debris campaign using existing sensors in the SSN from October 11 – November 8, 1994 (*1994 Space Debris Campaign Final Report*, 1995). The campaign was conducted in two phases. The first phase concentrated on detecting new objects while the second phase emphasized follow up tracking (although many additional objects were detected during Phase 2). Over 1100 element sets were added to the analyst list during the campaign although 350 of these were later identified as duplicates or as previously known objects. This left about 800 unique new objects tracked during the campaign. The campaign required special, manpower intensive, operating procedures to maintain the orbits of these objects. For instance, more than 40% of the new objects detected in the campaign were in high eccentricity orbits ( $> 0.1$ ). Orbits for these objects are more difficult to maintain than circular orbits because there are fewer sensor viewing opportunities. Additionally, the campaign specifically looked for low inclination orbits where normal SSN coverage is sparse.

When the campaign ended and the SSN returned to its normal operational procedures, the large majority of the 800 new objects were lost. Hence, about six months after the end of the campaign, most of the campaign objects were administratively removed from the analyst list of tracked objects (Devere, 2004).

## 7. OTHER COMPLETENESS ISSUES

There are other issues in addition to probability-of-detection that affect the completeness of measurements. For ground-based sensors, the latitude of the detection volume limits the inclinations that can be sampled. (Conversely, objects with inclinations which are equal to or slightly greater than the latitude of the detection volume are more likely to pass through the field-of-view.) Since the U.S. SSN (as well as the Russian network) has very few sensors located near the equator, low inclination orbits are, in all probability, under-sampled. Similarly, orbits with perigees that remain in the southern hemisphere for long periods of time are also likely under-sampled.

Returned surfaces are limited by altitude of their deployed orbits. In addition, they are valid only for the time they were deployed.

Another consideration is that even when an object is detected, information on the object may be incomplete. For staring measurements such as Haystack, orbital objects are in the field-of-view for a very short period of time. Without follow-up measurements, such as made by Cobra Dane, no information on eccentricity can be made. Optical measurements lack range information so that in order to estimate altitude, circular orbits must be assumed.

## 8. COMBINING DATA SETS

It is clear that no single measurement system provides complete information on the orbital debris environment. Issues associated with probability-of-detection can be overcome by combining measurements from many different systems. Fig. 4 shows data collected from Haystack and HAX radars during 2002 for the altitude range 850-1000 km. These two radars are co-located and share much of their real-time control and data processing equipment although they operate at different frequencies using different antennas. Haystack has higher sensitivity than HAX as well as a smaller beamwidth (0.58 for Haystack vs. 0.1 for HAX). Because they are collocated, they sample the same distribution of orbiting objects (although they are not operated simultaneously). The only adjustment to the count rate needed for these two radars is to scale them to the same beamwidth. In this figure, the HAX beamwidth has been scaled to match Haystacks. The

measured detection rate from the two systems is nearly identical above about 3 cm diameter. Below this size, the probability of detection begins to fall off for HAX while it remains near 100% for Haystack for sizes as small as 6 mm diameter.

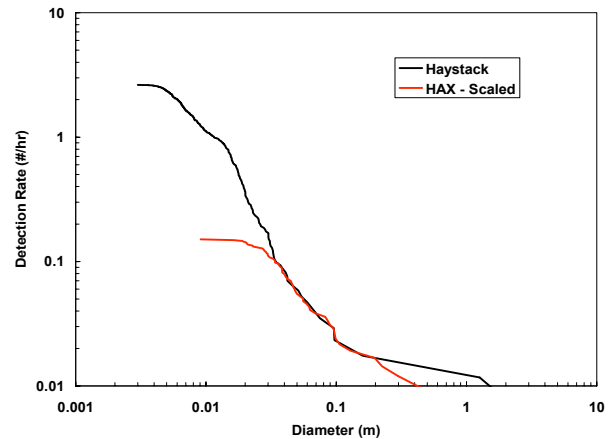


Figure 4. Haystack and HAX data for 850-1000 km altitude collected in 2002. HAX detection rate is scaled to match the collection area of Haystack.

It is more difficult to combine information from sensors that are not co-located or that are otherwise dissimilar.

For instance, combining information from LDEF with information from the Hubble solar arrays (both returned surfaces) necessitates accounting for differences in the epoch of their exposures to space as well as differences in altitudes.

Resolving differences in measurement type is even more difficult since no method directly measures debris size (with the possible exception of aerogel capture cells). For returned surfaces, debris size is inferred by measuring hole or crater size. Optical telescopes measure brightness and must infer an albedo in order to estimate size. Radars measure radar cross section (RCS) and relate to size through NASA's SEM or some other model. Relating debris size to what is actually measured by any system type is a very active area of research.

Fig. 5 shows our best attempt at combined measurements from many disparate sensors for the altitude of 500 km. Measurements from the SSN, HAX, Haystack, and Goldstone show remarkable consistency since they are all ground based radar measurements taken during the same time period. Although there is some scatter in the data from the sample return missions, there is still good consistency among the *in situ* measurements as well as the between these and the ground based measurements.

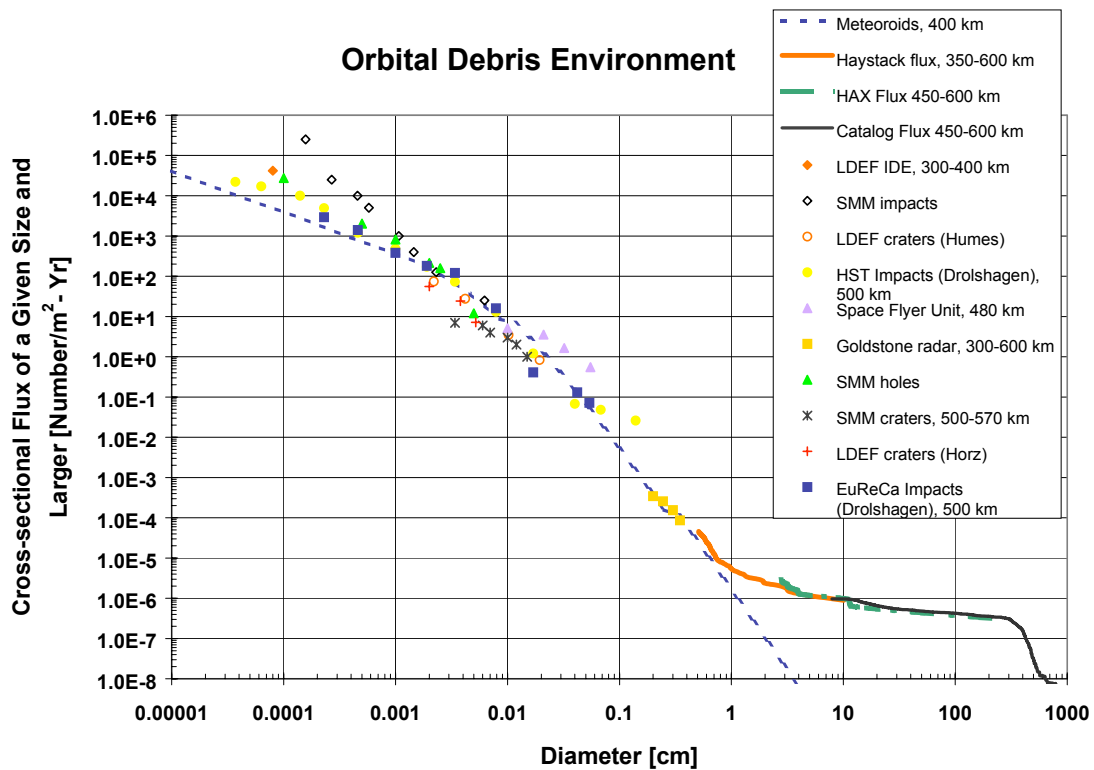


Figure 5. Combined measurements from many disparate sensors for the altitude of 500 km.

## 9. CONCLUSIONS

Although almost the entire debris size spectrum is represented in Fig. 5, issues like under-sampling of certain orbits such as those with low inclination and high eccentricity cannot be reliably accounted for. Additional sensors are needed which can provide complete coverage of all orbits. NASA is attempting to address the low inclination population by utilizing the Ground Based Radar-Prototype radar located at 9° N Lat. on the island of Kwajalein in the Pacific. Additionally, in cooperation with the Air Force Maui Optical & Supercomputing System (AMOS), NASA hopes to deploy the Meter Class Autonomous Telescope (MCAT) at Kwajalein. A unique operating mode for this telescope should overcome the meteor contamination issue. Only with continued efforts such as these will the current gaps in measurements be filled in so that our knowledge of the debris environment can be described as “complete.”

## 10. REFERENCES

- 1994 Space Debris Campaign Final Report, SenCom Corp., Colorado Springs, CO, 1995.
- Africano, J. L., et al. *Liquid Mirror Telescope Observations of the Orbital Debris Environment: October 1997- January 1999*, JSC-28826, 1999.
- Devere, G. T. Air Force Satellite Assessment Center, Personal Communication, 2004.

Foster, J. L., et al. Detections of Small Cross Section Orbital Debris with the Haystack Radar, Accepted for publication in *Adv. Space Res.*, 2005.

Ricker W. R., The Concept of Confidence or Fiducial Limits Applied to the Poisson Frequency Distribution, *J. American Statistical Assn.* Vol. 32, 349-356, 1937.